Available online at www.sciencedirect.com
SCIENCE DIRECT®
Microporous and Mesoporous Materials 78 (2005) 83–89
MICROPOROUS AND MESOPOROUS MATERIALS
www.elsevier.com/locate/micromeso

Preparation and characterization of thermally stable porous ceria aggregates formed via a sol–gel process of ultrasonically dispersed cerium(IV) isopropoxide

Kamal M.S. Khalil *, Leena A. Elkabee, Brian Murphy

Department of Chemistry, Faculty of Science, UAE University, P.O. Box 17551, Al-Ain, United Arab Emirates

Received 10 December 2003; received in revised form 23 September 2004; accepted 28 September 2004
Available online 24 November 2004

Abstract

Porous ceria aggregates of submicron size were obtained from cerium(IV) isopropoxide via a two-step sol–gel process. In the first step, dispersion of the cerium(IV) isopropoxide in isopropanol media was achieved by ultrasonic radiation, where limited hydrolysis occurred and resulted in the formation of a stable dispersant gel phase. In the second step, the resultant dispersions were mixed under stirring with a neutral (water–isopropanol) or basic (aqueous ammonium hydroxide–isopropanol) solution where complete hydrolysis took place. The structural and morphological characteristics of the uncalcined (dried at 120 °C) and the calcined (at 650 °C for 3 h in static air) materials were investigated by TGA, XRD, FTIR, SEM and nitrogen adsorption techniques. It was found that the type of media affected both the particle texture and the morphology. For the calcined materials, porous textural aggregates with specific surface areas of 33.1 and 44.2 $m^2 g^{-1}$ were measured for the materials obtained via neutral and basic preparations. In addition, smaller particle size, higher mesoporous area and higher aggregation morphology were found for the material produced from the preparation in base. The preservation of surface area and porosity for the calcined materials was explained as a result of the aggregated morphology which was greater for the material produced in base.

Keywords: Ceria; CeO_2; Cerium(IV) isopropoxide; Thermal stability; Sol–gel; Porous material

1. Introduction

Ceria, CeO_2, is one of the most important catalytic materials that can play multiple roles owing to its ability to release and uptake oxygen under catalytic reaction conditions with the preservation of its fluorite structure [1,2]. However, the catalytic efficiency of ceria may be reduced at elevated temperatures due to sintering and loss of surface area [3]. For example, thermal stability is a critical issue in determining the promoting and metal supporting functions of CeO_2 in its catalytic applications in the three way catalytic process [4]. For this reason, significant efforts have been made by industry in trying to find ways to improve the thermal stability either by alternative methods involving the synthesis of ceria or by modifying the different types of stabilizers involved [4]. A large number of studies have been reported in the literature for the synthesis and modification of ceria-based materials with different stabilizers [5]. In order to prepare pure ceria with improved textural and thermal stability several synthetic modifications have been reported in the literature, which include: a surfactant-assisted method [3,6,7], a coupling route of homogenous precipitation with micro-emulsion [8], reversed micelles [9], precipitation [10] by a mimic method [11]

* Corresponding author. Permanent address: Department of Chemistry, Faculty of Science, South Valley University, Sohag, P.O. Box 82524, Egypt. Tel.: +971 50 4499 487; fax: +971 3 7671 291 (at UAE).
E-mail address: kamalk@uaeu.ac.ae (K.M.S. Khalil).

1387-1811/$ - see front matter © 2004 Elsevier Inc. All rights reserved.
doi:10.1016/j.micromeso.2004.09.019

and high-intensity ultrasound irradiation without thermal post-treatment [12].

The sol–gel technique based on the hydrolysis of alkoxides is one technique which has been successfully employed for the preparation of a large number of single as well as mixed metal oxides [13,14], and metal oxides with good thermal stability [15,16]. However, to the best of the authors' knowledge, use of this technique has not previously been reported in the literature for the preparation of pure ceria material, probably due to limited solubility of alkoxides in an alcoholic medium. As a result, the aim of this present work is to report a two step sol–gel process in which cerium(IV) isopropoxide was dispersed in isopropanol by the aid of ultrasonic radiation to overcome the solubility problem. The hydrolysis reaction took place in neutral or in basic isopropanol media, followed by subsequent aging, drying and calcination for 3 h at 933 K. Textural characteristics of the ceria powders obtained via this method were characterized using thermogravimetric analysis (TGA), X-ray diffraction (XRD), Fourier transfer infrared spectroscopy (FTIR), nitrogen physisorption and scanning electron microscopy (SEM), respectively.

2. Experimental

2.1. Parent chemicals

Cerium(IV) isopropoxide, $Ce[OCH(CH_3)_2]_4 \cdot C_3H_7OH$, powder, product of Alfa Aesar, Isopropanol, 99.7+%, $(CH_3)_2CHOH$ (water contents <0.05%), product of Merck, and ammonium hydroxide, NH_4OH (25% NH_3), 99.99%, product of Merck, were used as-received.

2.2. Preparation of ceria materials

At room temperature, 0.01 mol of cerium(IV) isopropoxide was dispersed in 50 ml of isopropanol by the aid of ultrasonic radiation in a conventional small bench top ultrasonic bath (power 100 W) for a period of 10 min. During this process some hydrolysis occurred due to traces of water (<0.05%) present in the isopropanol. This resulted in a translucent stable gel like dispersant. The resultant dispersion was transferred into a 600 ml beaker containing 207.0 ml of absolute alcohol and 155 ml of water for the *neutral* preparation (or 155 ammonia solution 25%, for the *basic* preparation). A white opaque sol was formed instantaneously. The solution was magnetically stirred at ≈400 rpm and the sol was kept under stirring for 1 h. The resultant solution was covered with a glass watch cover and aged for 1 week, at room temperature. The cake thus stilled was filtered off using Whatman filter paper Number 41. The resultant materials, without washing, were left to dry overnight at 60 °C and allowed to dry further at 120 °C for 24 h. The resultant materials are termed as Ceria-N120, and Ceria-B120 for the neutral and the basic preparations respectively. Portions of the Ceria-N120, and Ceria-B120 materials were calcined in a muffle furnace at 650 °C for 3 h in a static atmosphere. The calcined materials which are powders, are named after their respective precursors as Ceria-N650, Ceria-B650 for the neutral and the basic preparations.

2.3. Characterisation

Thermogravimetric analysis (TGA). TGA was carried out using a thermogravimetric analyzer, TA Instruments GA 2950, (USA). A ceramic sample boat was used. Samples weighing 10.0 ± 0.1 mg were heated in a ceramic sample boat up to 900 °C at 10 °C min^{-1} and in a stream (40 ml min^{-1}) of nitrogen gas or air.

Fourier transform infrared (FTIR) spectroscopy. FTIR spectroscopy for the samples was carried out using the normal KBr disc technique using a Fourier transform infrared spectrophotometer, Nicolet FTIR Magna-IR 560 system (USA), in the range 4000–400 cm^{-1}, with 40 scans and a resolution of 4 cm^{-1}.

X-ray diffraction (XRD): XRD patterns were obtained using a Philips 1840 diffractometer at room temperature using CuK_α radiation. Diffraction patterns were obtained with Ni-filtered CuK_α radiation ($\lambda = 0.15418$ nm). The resultant patterns matched with standard data of CeO_2 [17] for the purpose of phase identification. The crystallite size of the ceria powder was estimated from the Scherrer equation [18]:

$$D = 0.9\lambda/(\beta \cos\theta)$$

where D is the crystallite size; λ is the wavelength of the incident X-ray; θ is the angle of diffraction for the 1 1 1 line and β is the half-width of the peak which was measured graphically.

Scanning electron microscopy (SEM). SEM micrographs were obtained, using a Jeol microscope Model JSM-5600. The samples were coated with gold before investigation.

Nitrogen gas adsorption. Nitrogen adsorption/desorption isotherms at 77 K were measured using a model ASAP 2010 Micromeritics Instrument Corporation, USA. Prior to measurement, all samples were degassed for 2 h at 150 °C to 0.1 Pa. The specific surface area, S_{BET} was calculated using the BET equation [19]. The porosity distribution (>2 up to >100 nm) was generated from the adsorption branches of the isotherms by the BJH analysis using the software of the instrument. An assessment of microporosity was found using the Harkins–Jura correlation [20] for a t-plot. The t-plot surface areas, S_t, were calculated from the analysis of the gradients of the t-plots using standard methods. The micropore surface area, S_{mic}, corresponding to the gas

condensed in micropores, was calculated using the expression, $S_{mic} = S_{BET} - S_t$.

3. Results and discussion

3.1. Thermogravimetry

TGA of the uncalcined powder material Ceria-N120, in a flow of nitrogen gas or air is shown in Fig. 1. Weight loss amounts of 12.43% and 12.27% respectively were recorded upon heating from room temperature (rt) to 900 °C. The TGA thermogram carried out in a flow of nitrogen gas, Fig. 1, exhibits three general TGA peaks at 72, 245–371 and 694, corresponding to the presence of three main regions of weight loss. In the air flow, Fig. 1, three TGA peaks corresponding to the presence of three main weight loss regions were also observed. However, the region limits were shifted toward lower temperatures, and the peaks are more resolved for this analysis with maxima at 73, 221 and 750 °C respectively. Examination of the two curves for the Ceria-N120 material in either a nitrogen gas or air flow shows that the main difference produced by the atmosphere appears in the second weight loss region, >150 to ~600 °C, where a faster weight loss in the flow of air than in the flow of nitrogen gas was observed. However, the two curves are superimposed near 700 °C.

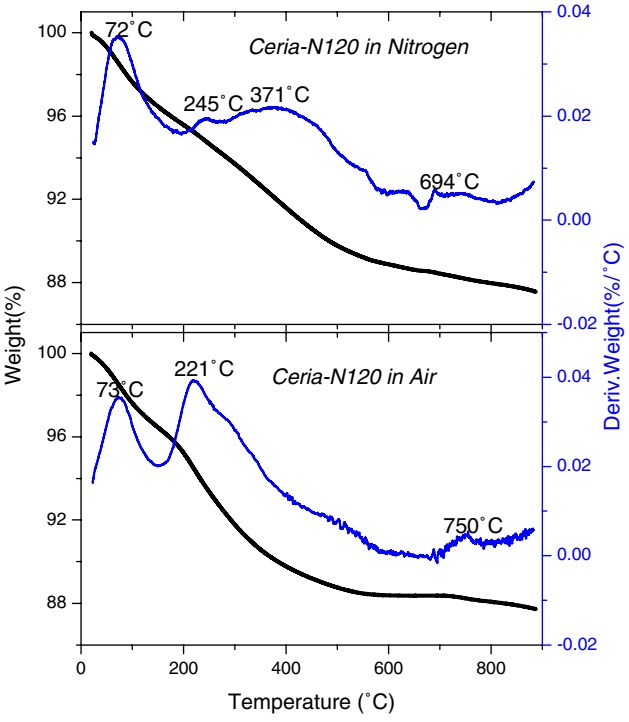

Fig. 1. TGA and DTG curves of the CeriaN-120 material carried out in (a) flow of nitrogen gas (top), and (b) flow of air (bottom).

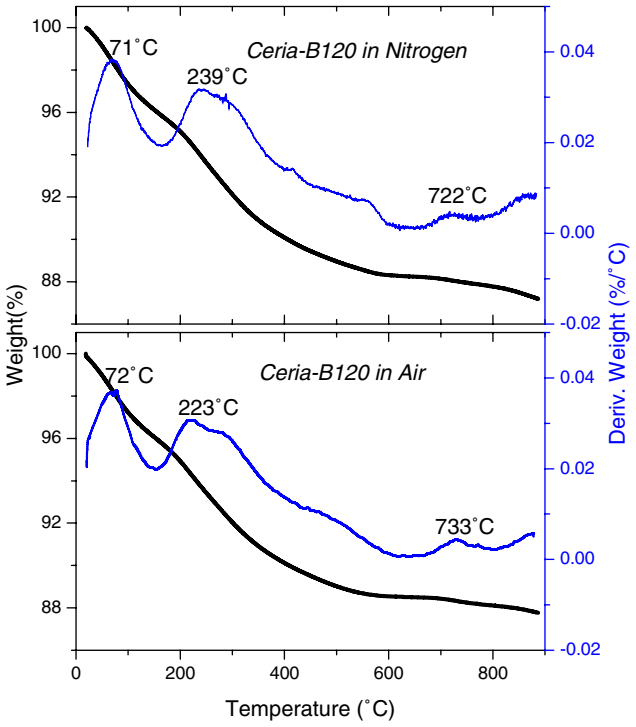

Fig. 2. TGA and DTG curves of the CeriaB-120 material carried out in (a) flow of nitrogen (top), and (b) flow of air (bottom).

TGA curves for the uncalcined powder material Ceria-B120, in a flow of nitrogen gas and air are shown in Fig. 2. Weight losses of 12.80% and 12.24% respectively in nitrogen and air were observed. Three DTG peaks at 71, 239 and 722 °C in nitrogen, and at 72, 223 and 733 °C in air were observed, see Fig. 2. Comparison between the two curves obtained for the Ceria-B120 material in flows of nitrogen or air generally showed similar features to the case of Ceria-N120. However, the curves in nitrogen and in the air flow are much more analogous indicating a lesser dependence on the type of the atmosphere (nitrogen or air flow) in the case of Ceria-B120.

Therefore, the TGA results for Ceria-N120 and Ceria-B120 can be discussed as follows. Through the first weight loss region, desorption of physically adsorbed water and/or organic solvent occurs. The second weight loss region may be assigned to the decomposition and/or combustion of residual organic species (see FTIR results below), which is more pronounced for Ceria-N120 than for Ceria-B120. The small percent weight loss observed in the third weight loss region may be due to the decomposition of some residual adsorbed species and/or oxygen loss at high temperature.

3.2. X-ray diffraction

XRD patterns for the dried hydrolysis products are very broad with low intensity and with a low signal to noise ratio. Fig. 3 shows X-ray diffraction patterns for

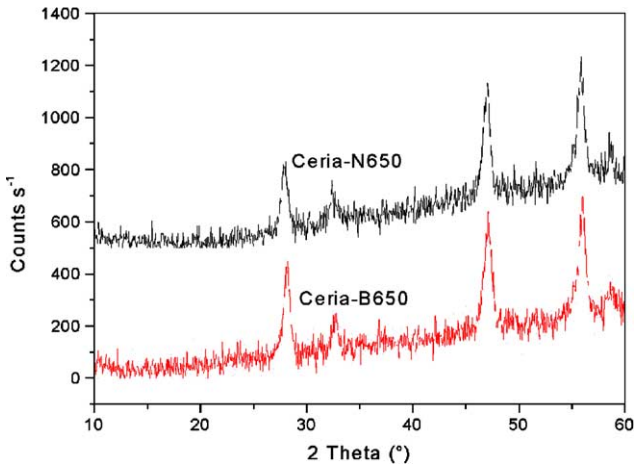

Fig. 3. XRD patterns for the calcined CeriaN-650 and CeriaB-650 materials.

the 650 °C calcined materials. Hence, well-defined peaks of better signal/noise ratio are observed which match those reported previously for ceria [cards no. 34-394, JCPDS]. It should also be stated that no other phases were detected in the examined materials.

3.3. FTIR spectra

Fig. 4 shows the FTIR spectra of Ceria-N120 (uncalcined) and Ceria-N650 (calcined), respectively. The spectrum for Ceria-N120 shows a group of strong intense bands at 3423 cm^{-1}, 1546 cm^{-1} and in the region, 1354–1382 cm^{-1}. The spectrum also shows two other groups of peaks of lower intensity; one group at 2974, 2921 and 2863 cm^{-1} and the other group with peaks at 1054, 944 and 851 cm^{-1}. In light of the proposed assignments of such peaks in other similar systems [3,6,21] the observed bands can be assigned as follows: the intense band at 3423 cm^{-1} corresponds to the ν(O–H) mode of (H-bonded) water molecules. The group of peaks of weak intensity, centred at 2974, 2921 and 2863 cm^{-1} are assigned to the ν(C–H) mode of organic moieties. The low intensity associated with this group of peaks is indicative of the low content of organic material in Ceria-N120. The strong broad peak centred at 1546 cm^{-1} may be due to the $\nu_{as}(COO^-)$ and $\nu_a(COO^-)$ modes. The strong broad peak, centred between 1354 and 1382 cm^{-1} may be partially assigned to the $\delta(CH_3)$ mode of the residual organic moieties. The peak at 1054 cm^{-1} of low intensity may be assigned to the stretching mode, ν(C–O) of the OPr^i group. A similar assignment was made previously by Maggio et al. [21] for C–O of OBu^n in a Ce–Zr dried gel. The broad band below 700 cm^{-1} is due to the envelope of the phonon band of the metal oxide network.

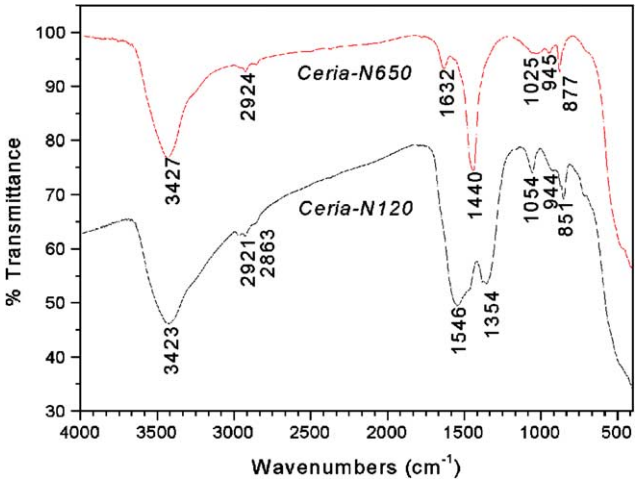

Fig. 4. FTIR spectra for the CeriaN-120 and its calcination product CeriaN-650.

The spectrum for Ceria-N650, Fig. 4, shows a group of peaks closely related to those observed for its parent material. As reported previously by Lyons et al. [22], on calcination, there is a dramatic decrease in the intensity of the typical broad features of the uncalcined species. The 3427 and 1632 cm^{-1} peaks are assigned to the ν(O–H) mode of (H-bonded) water molecules, and δ(OH), respectively. The latter band is not resolved in the spectrum of Ceria-N120, probably due to its overlap with the other bands that gives rise to the broad nature of the 1546 cm^{-1} peak. Two other well-resolved peaks are observed however for the Ceria-N650 spectrum at 1440 and 877 cm^{-1}. Thus, there is clear evidence of the presence of carbonate in the spectrum. In previous work [23] Binet et al. reported the presence of adsorbed species from CO_2 adsorption on unreduced ceria at room temperature, including hydrogen carbonates and carbonates. The spectral features (both in terms of intensity and approximate wavenumber) shown in Fig. 4 are very similar to those reported [22] in relation to the adsorbed bidentate carbonate.

The FTIR spectra of Ceria-B120 (uncalcined) and Ceria-B650 (calcined) are similar to the neutral preparation, which are not shown here. However, the 1440 cm^{-1} peak due to carbonate is much more pronounced for the Ceria-B650 than for the Ceria-N650 sample. However, it has been suggested previously that carbon dioxide is an inevitable adsorbent on ceria surfaces at rt and is indicative of high surface basicity of surface O^{2-} ions for ceria [23]. This suggests that surface carbonate species play an important role in the preservation of surface area and porosity of the basic prepared material than the neutral one, see below.

3.4. Nitrogen adsorption

The isotherms for nitrogen adsorption/desorption for the two calcined materials are shown in Fig. 5. According to the original IUPAC classification [24], the

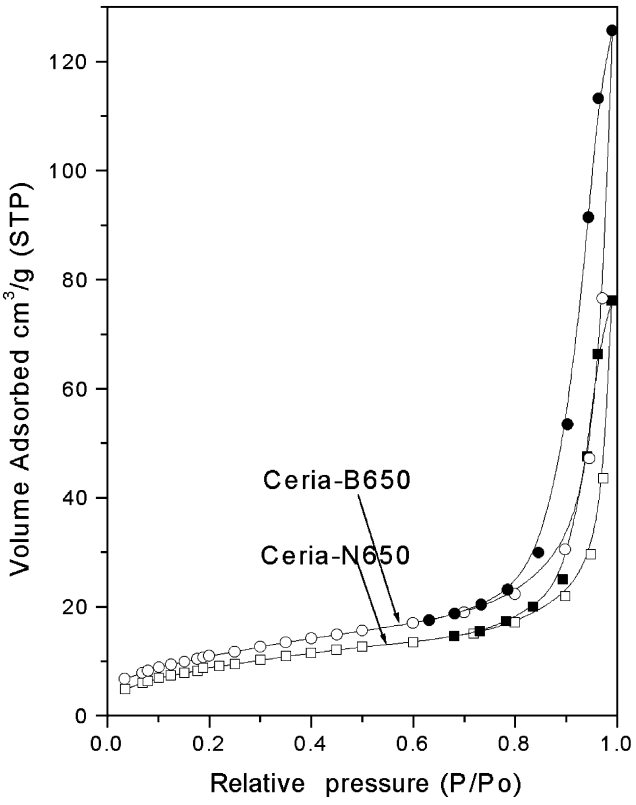

Fig. 5. N_2 adsorption/desorption isotherms for the CeriaN-650 and CeriaB-650 materials.

isotherms are similar in behaviour to type II type isotherms with some contribution from type IV type isotherms. The loops are relatively narrow especially for the Ceria-N120 material; the adsorption and desorption branches are almost vertical and parallel. The loops can therefore be classified as Type H1 hysteresis. Additionally, according to the recent classification for the adsorption isotherms [25], the isotherms are of mixed Type IIa and Type IVb isotherms.

The assigned classifications indicate monolayer–multilayer adsorption on an open, stable external surface of powder. The isotherms show delayed location for the adsorption branch, which is governed by the delayed nitrogen condensation process due to wide porosity. However, as the nitrogen condensation process occurs at relatively higher p/p_0 for the Ceria-N650 material than that for the Ceria-B650 material, a wider pore size can be expected for the former.

Textural characteristics including surface area, S_{BET}, external surface area, S_t, micro-pore area, S_{mic}, along with the average particle size for the test materials are cited in Table 1. The table indicates that the Ceria-B650 material has a higher surface area, S_{BET}, of $41.2\,m^2g^{-1}$ compared to $33.1\,m^2g^{-1}$ for the corresponding Ceria-N650 material. Moreover, a lower contribution of microporosity was found for Ceria-B650 ($14.6\,m^2g^{-1}$ out of $41.2\,m^2g^{-1}$ total surface area) than for Ceria-N650 ($15.0\,m^2g^{-1}$ out of $33.1\,m^2g^{-1}$ total surface area). Table 1 also compares the present results with some other reported ceria materials from the literature.

3.5. Electron microscopy

SEM micrographs for the Ceria-N120 and Ceria-B120 precursor materials are shown in Fig. 6(a) and (b) respectively. The general morphology of the precursor obtained in neutral media, Ceria-N120, showed a case of porous aggregates of submicron to micron size. The aggregates are not uniform but they are composed of relatively equiaxed finer primary particles and show clear signs of porosity. However, the morphology of the precursor obtained in basic media, Ceria-B120, showed aggregates of smaller size, composed of highly cross-linked primary particles. Large fractions of the sample are present as free small clusters/and or primary particles.

SEM micrographs for the Ceria-N650 and Ceria-B650 precursor materials are shown in Fig. 7(a) and (b) respectively. Fig. 7(a) shows that Ceria-N650 is composed of many isolated desecrate particles and small size aggregates. This indicates a dramatic change in the material morphology (in comparison to its precursor, Ceria-N120). Such isolated desecrate particles and small size aggregates morphology reduces mesoporosity upon packing resulting in a lower surface area. However, for Ceria-B650, some primary aggregates consolidate with each other. Generally, the primary

Table 1
Textural characteristics: surface area, S_{BET}, external surface area, S_t, and micropore area S_{mic}, pore diameters and particle size for the test materials calcined at 650 °C in air for 3 h

Material	S_{BET} (m^2g^{-1})	c_{BET}	S_t (m^2g^{-1})	S_{mic} (m^2g^{-1})	Pore diameter (nm)		Particle size (nm)
					Average	BJH	
Ceria-N650	33.1	38.0	18.1	15.0	12.0	16.0	41
Ceria-B650	41.2	45.5	26.6	14.6	17.0	21.5	34
Ceria-973[a]	32.9	–	–	–	–	–	20.9
Ceria-650C[b]	16.9	68.1	–	–	–	–	–

[a] Data from Lundberg et al. [7].
[b] Data from a sample made by calcinations of cerium oxalate for 3 h at 650 °C.

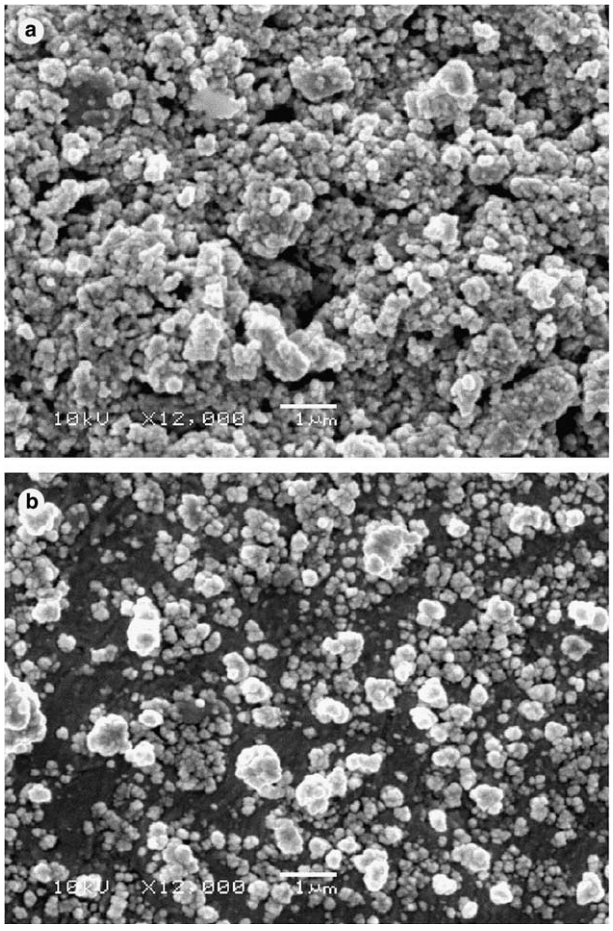

Fig. 6. Scanning electron micrographs of the uncalcined materials (a) CeriaN-120, and (b) CeriaB-120.

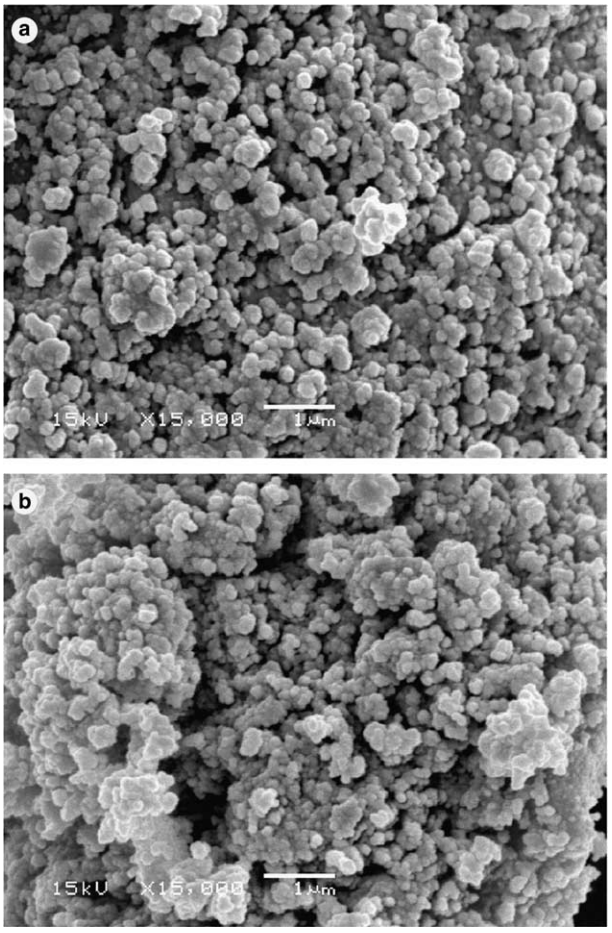

Fig. 7. Scanning electron micrographs of the calcined materials (a) CeriaN-650, and (b) CeriaB-650.

aggregates consolidate together at low coordination numbers giving rise to a more porous texture of higher surface area.

The above results show that it is possible to form porous ceria materials with potential catalytic applications from cerium(IV) isopropoxide via a simple sol–gel process that overcomes the inherent solubility problem of cerium(IV) isopropoxide. In addition, this method can be extended to other "alcohol-insoluble" transition element alkoxides, where the solubility in alcoholic media limits their application in the sol–gel process. The surface area and porosity of the sol–gel derived from the ceria materials are very satisfactory and suggest good thermal stability in terms of the preservation of surface area and porosity after calcinations for 3 h at 650 °C. In general, the sol–gel method has always been criticized in relation to two aspects. First, the contamination with organics through processing has been a negating factor in this method. In addition, the ease of sintering at high temperature despite the good surface area, which may have been obtained at low calcination temperatures has also been seen to be a disadvantage in the application of the method in this area. The present results (TGA and FTIR) have shown however that most of the organic impurities have been removed (and/or oxidized) relatively easily from the ceria surface due to the oxidizing nature of the ceria surface. Furthermore, the material processed in the neutral medium yields a good surface area of $33.1\,m^2\,g^{-1}$. A higher surface area of $41.2\,m^2\,g^{-1}$ was obtained for the material processed in the basic media. This suggests that good textural properties can be obtained in neutral media, and this can be further improved by conducting the hydrolysis in the presence of a high ammonium hydroxide concentration (ammonium hydroxide: alkoxy ratio, 20:1). It should be noted that the ammonium hydroxide ratio implemented in the present study is similar to that used by Stöber et al. [26] to produce spherical silica particles via hydrolysis of TEOS (this is not the case for ceria due to many reasons). Nevertheless, similar to the case of TEOS, it can be argued that a high ammonium hydroxide concentration helps in the removal of the terminal alkoxy groups, increases the surface hydroxylation, and protects the particle against fast sedimentation during the settling processes. The effect of ammonium hydroxide can be seen by comparing the micrographs

of Ceria-N120 and Ceria-B120, Fig. 6(a) and (b) respectively, where isolated particles and small aggregates are formed in the case of ammonium hydroxide. The presence of very many small particles for the material processed in the presence of ammonium hydroxide indicates that the nucleation and growth processes were largely affected. However, no trace of ammonia was observed from the FTIR spectra of the dried material Ceria-N120. It can be suggested that the ammonia probably oxidized on the surface of ceria and was removed in the early stages of the drying process. SEM micrographs indicated that both of the calcined materials are composed of porous aggregates, but to different degrees however. The virtue of this aggregated porous morphology can be helpful too in limiting particle growth within the initial aggregate border upon calcinations at high temperature. Finally, it has been reported that carbonate ions present in CeO_2 have a stabilizing role on the texture [27]. Hence, it can be argued that increasing the surface hydroxylation (in the presence of ammonium hydroxide) of the particles and in the presence of carbonate species, stabilizes the aggregated particles against sintering at a lower temperature. For this reason, better stability was obtained for the calcined material processed in a basic rather than in a neutral medium.

4. Conclusion

In this work, porous ceria aggregates of submicron size were obtained from cerium(IV) isopropoxide via a two-step sol–gel process. It was found that the type of media affected both the particle texture and the morphology. For the calcined materials, porous textural aggregates with specific surface areas of 33.1 and $44.2\,m^2\,g^{-1}$ were measured for the materials obtained via neutral and basic preparations. In addition, smaller particle size, higher mesoporous area and higher aggregation morphology were found for the material produced from the preparation in base. The preservation of surface area and porosity for the calcined materials was explained as a result of the aggregated morphology which was greater for the material produced in base.

References

[1] A. Trovarelli, Catal. Rev. Sci. Eng. 38 (1996) 439.
[2] A. Trovarelli (Ed.), Catalysis by Ceria and Related Material, Imperial College Press, London, 2002.
[3] R. Cracium, W. Daniell, H. Knozinger, Appl. Catal. A: Gen. 230 (2002) 153.
[4] J. Kaspar, P. Fornasiero, M. Graziani, Catal. Today 50 (1999) 285.
[5] G. Adachi, T. Masui, in: A. Trovarelli (Ed.), Catalysis by Ceria and its Related Materials, Imperial College Press, London, 2002, pp. 51–83, and references therein.
[6] D. Terribile, A. Trovarelli, J. Llorca, C. de Leittenburg, G. Dolcetti, J. Catal. 178 (1998) 299.
[7] M. Lundberg, B. Skarman, F. Cesar, L.R. Wallenberg, Micropor. Mesopor. Mater. 54 (2002) 97.
[8] Y. He, B. Yang, G. Cheng, Mater. Lett. 57 (2003) 1880.
[9] T. Masui, K. Fujiwara, K. Machida, G. Adachi, Chem. Mater. 9 (1997) 2197.
[10] L.A. Bruce, M. Hoang, A.E. Hughes, T.W. Turny, Appl. Catal. A 134 (1996) 351.
[11] J.G. Li, T. Ikegami, J.H. Lee, T. Mori, Acta Mater. 49 (2001) 419.
[12] J.C. Yu, L. Zhang, J. Lin, J. Coll. Interface Sci. 260 (2003) 240.
[13] J.D. Wright, N.A.J.M. Sommerdijk, Sol–Gel Materials Chemistry and Applications, Taylor & Francis Books Ltd., London, 2001.
[14] C.J. Brinker, G.W. Scherer, Sol–Gel Science, The Physics and Chemistry of Sol–Gel Processing, Academic Press, New York/London, 1989.
[15] K.M.S. Khalil, J. Catal. 178 (1998) 198.
[16] K.M.S. Khalil, M.I. Zaki, Powder Technol. 120 (2001) 256.
[17] JCPDS, International Centre for Diffraction Data, CD, 1996.
[18] H.P. Klug, L.E. Alexander, X-ray Diffraction Procedure for Polycrystalline and Amorphous Material, Wiley, New York, 1974.
[19] B. Brunauer, P.H. Emmett, P.H.E. Teller, J. Am. Chem. Soc. 60 (1938) 309.
[20] W.D. Harkins, G.J. Jura, J. Chem. Phys. 11 (1943) 431.
[21] R.D. Maggio, R. Campostrini, G. Guella, Chem. Mater. 10 (1998) 3839.
[22] D.M. Lyons, K.M. Ryan, M.A. Morris, J. Mater. Chem. 12 (2002) 1207.
[23] C. Binet, M. Daturi, J.C. Lavelly, Catal. Today 50 (1999) 207, and references therein.
[24] International Union of Pure and Applied Chemistry, IUPAC, Pure Appl. Chem. 57 (1985) p. 603.
[25] F. Rouquerol, J. Rouquerol, K. Sing, Adsorption by Powders and Porous Solids, Academic Press, London, 1999, p. 440.
[26] W. Stöber, A. Fink, E. Bohn, J. Coll. Interface Sci. 26 (1968) 62.
[27] V. Perrichon, A. Laachir, S. Abouarnadasse, O. Touret, G. Blanchard, Appl. Catal. A: Gen. 129 (1995) 69.